

# Natural & unnatural-parity contributions in electron-impact ionization of laser-aligned atoms.

Andrew James Murray<sup>1\*</sup>, James Colgan<sup>2</sup>, Don Madison<sup>3</sup>, Matthew Harvey<sup>1</sup>, Ahmad Sakaamini<sup>1</sup>, James Pursehouse<sup>1</sup>, Kate Nixon<sup>4</sup> & Al Stauffer<sup>5</sup>

<sup>1</sup> Photon Science Institute, School of Physics & Astronomy, University of Manchester, Manchester M13 9PL, UK

<sup>2</sup> Theory Division, Los Alamos National Laboratory, Los Alamos, 87545 NM, USA

<sup>3</sup> Physics Department, Missouri University of Science and Technology, Rolla, Missouri 65409, USA.

<sup>4</sup> School of Sciences, Wolverhampton University, Wolverhampton, UK, WV1 1LY.

<sup>5</sup> Dept. of Physics and Astronomy, York University, Toronto, Ontario, Canada.

\* Andrew.Murray@manchester.ac.uk

**Abstract.** Differential cross section measurements from laser-aligned Mg atoms are compared to theoretical calculations using both time dependent and time-independent formalisms. It is found that both natural and unnatural parity contributions to the calculated cross sections are required to emulate the data when the state is aligned out of the scattering plane.

## 1. Introduction.

Electron impact ionization processes play an important role in many areas of research, ranging from calculations of stellar and planetary atmospheres through to collision processes in plasmas and in lasers, lighting and Tokomaks. Measurements of the angular correlation between the scattered (initially incident) electron and the electron ejected following ionization then provides the most precise detail of the collision that occurs.

For atomic targets that are in their ground state, a Triple Differential Cross Section (TDCS) is then determined, which depends upon the energetics of the collision and the angular distribution of the detected electrons. By contrast, for atoms that are *pre-aligned* (e.g. using a continuous wave (CW) laser beam) prior to the collision, a further angle must be introduced that defines the initial target alignment. In this case a quadruple cross section is defined (QDCS) which depends upon the momentum of the incident electron  $\mathbf{k}_0$ , the scattered and ejected electron momenta  $\mathbf{k}_1, \mathbf{k}_2$  and the alignment angle of the target  $\mathbf{k}_T$ .

Theoretical models of the collision solve Schrödinger's equation for the interaction using either time-dependent or time-independent approaches. The time dependent model used here is from the Los Alamos group of James Colgan, and uses a close-coupling method to define the interaction. This is referred to as the TDCC model [1]. The time-independent models of Don Madison's group that are adopted here describe the collision using distorted waves, and include the effects of post-collisional interactions in different ways. These are referred to as the DWBA and 3DW models [2]. Full details of the different calculations can be found in the references from each of these groups.



In this report results are presented for electron-impact ionization of magnesium atoms that are excited and pre-aligned using CW laser radiation at 285.2965nm. Linearly polarized radiation excites the Mg atoms from the  $3^1S_0$  ground state to the  $3^1P_1$  state, and the energetics of the interaction are then exploited to only select ionization events from excited targets. The QDCS obtained from the measurements are then compared to that from ionization of atoms in the ground state, and are further compared to predictions from the different models.

## 2. QDCS measurements for magnesium (target aligned in the plane).

The first experiments detailed here adopt a geometry where the laser beam is incident orthogonal to the scattering (detection) plane, so that the alignment direction of the excited target remains in the scattering (collision) plane. This is shown in figure 1.

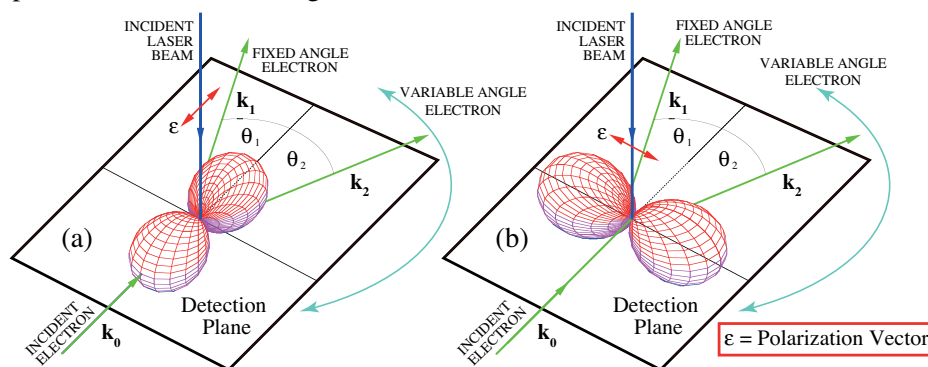


**Fig. 1.** Experimental geometry with the laser incident perpendicular to the scattering (detection) plane defined by  $(\mathbf{k}_0, \mathbf{k}_1, \mathbf{k}_2)$ . The P-state is shown aligned (a) along  $\mathbf{k}_0$  and (b) perpendicular to  $\mathbf{k}_0$ .

Under these conditions the QDCS depends upon the angles  $\theta_1$  and  $\theta_2$  as well as the state alignment direction  $\varepsilon$ . The experiments further constrained the kinematics so that  $\theta_1$  was fixed at  $30^\circ$  while both  $\theta_2$  and  $\varepsilon$  were varied. The incident electron had energy 47.65eV and both outgoing electrons were detected with an energy of 20eV.

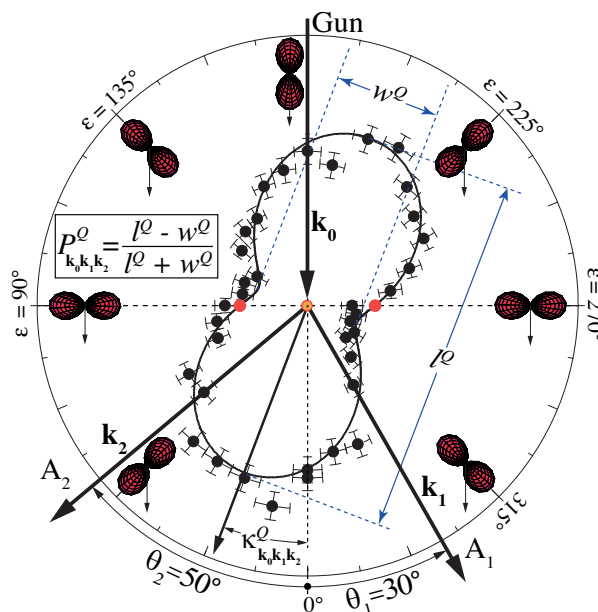


**Fig. 2.** The measured QDCS at fixed angles  $(\theta_1, \theta_2) = (30^\circ, 50^\circ)$  as a function of the alignment angle of the target state  $\varepsilon$ . The QDCS is then parameterized, as discussed in the text.

Figure 2 shows the results of this study, where  $\theta_2$  was fixed at  $50^\circ$  and the alignment angle of the target was varied around the scattering plane. The data show the expected symmetry as  $\varepsilon$  varied, allowing a parametric fit to be made to the QDCS as a function of the alignment angle. The parameters chosen were  $P_{k_0, k_1, k_2}^Q$  which defines the length to width ratio of the QDCS, and  $\kappa_{k_0, k_1, k_2}^Q$  which defines the angle of the major axis of the QDCS from the incident beam direction. These parameters were then used to compare to different models, as detailed in [3,4].

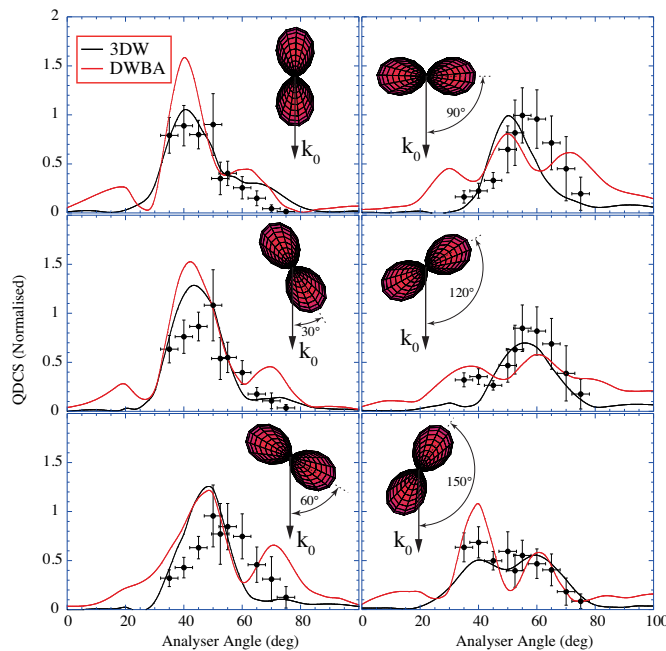


**Fig. 3.** The measured QDCS as a function of target alignment angle  $\varepsilon$  and scattering angle  $\theta_2$  for a fixed angle  $\theta_1 = 30^\circ$ , compared to the DWBA and 3DW time-independent calculations.

A further set of measurements varied both  $\theta_2$  and  $\varepsilon$ , allowing additional comparison with theory. A selection of data are shown in figure 3, compared to the calculations from Don Madison’s group [5]. Both DWBA and 3DW calculations are depicted, with the 3DW calculation showing better agreement with experiment in terms of the magnitude of the QDCS, and the number of peaks that are predicted.

**3. QDCS measurements for magnesium (target aligned out of the scattering plane).**

A second set of measurements was carried out with the laser beam input in a direction opposing the incident electron beam [6]. In this case the target could be aligned from in the plane to perpendicular to the plane as shown in figure 4.

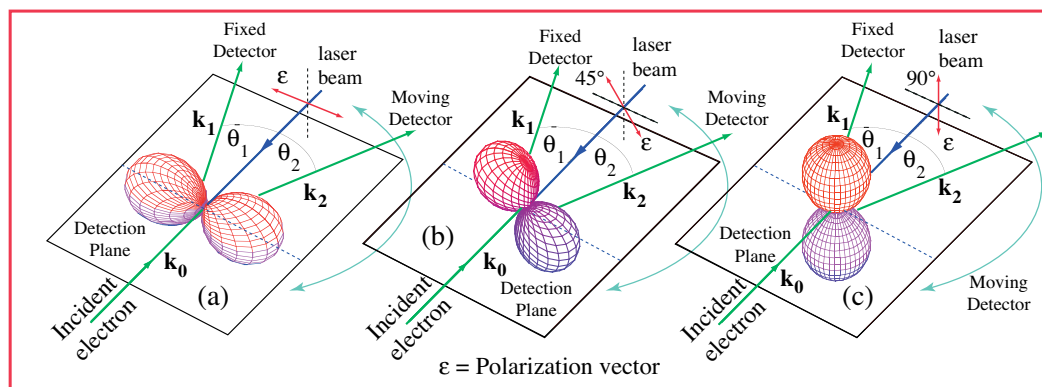


**Fig. 4.** Experimental geometry with the laser input in the direction  $-\mathbf{k}_0$ . In this case the excited target could be aligned from in-plane to perpendicular to the detection plane.

Once again the data can be compared to theory [7], and this is shown in figure 5 together with results from ionization of Mg atoms in the ground state (figure 5(a)). For the ground state all models predict the correct structure of the TDCS, with the 3DW model passing through all data points. By contrast, for the aligned target the models fail to predict the data accurately, and indeed the time-independent models predict that the QDCS for alignment perpendicular to the plane should be exactly zero for all scattering angles. This is in strong disagreement with the data, and also does not agree with the TDCC model. Since the QDCS in figure 5(d) is  $\sim 50\%$  of that when the target is aligned in the plane, there is clearly something missing in the DWBA and 3DW models for these kinematic conditions. The TDCC model *does* predict a finite cross section under these conditions.

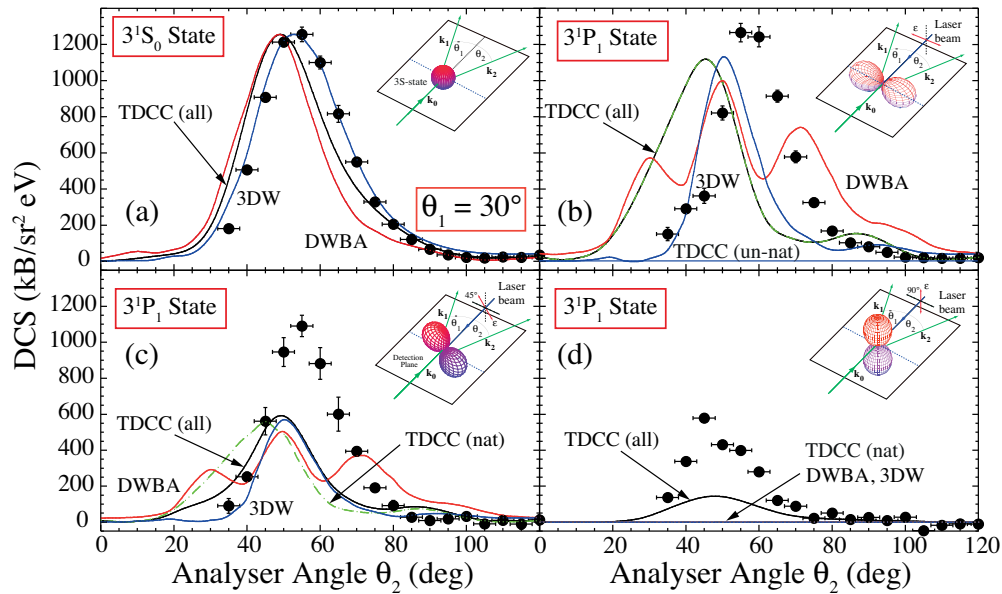


**Fig. 5.** Results with the laser input in the direction  $-\mathbf{k}_0$ , for (b) the P-state aligned in the plane, (c) for the state aligned at  $45^\circ$  to the plane and (d) when the state is aligned orthogonal to the plane. A comparison is also made to the TDCS from targets in the ground state in (a). TDCC (nat) shows the calculation with only natural parity terms, TDCC (un-nat) with only unnatural parity terms included, and TDCC (all) shows the calculation with both natural and unnatural parity terms. For full details see text.

#### 4. Natural and unnatural parity terms in the models.

The results in figure 5 show a clear difference between the models, with the full TDCC calculation (TDCC (all)) predicting a finite QDCS for alignment perpendicular to the plane, in contrast to the distorted wave models that predict the QDCS to be identically zero for all angles. This is found to arise from contributions of so-called *unnatural parity terms* that are included in the TDCC model, but which are absent in the DWBA and 3DW calculations [7].

To understand how these terms arise in the TDCC calculation, the QDCS can be written as an expansion over partial waves, so that the QDCS is given by:

$$QDCS(\mathbf{k}_0, \mathbf{k}_1, \mathbf{k}_2, \mathbf{k}_T) = \frac{w_l}{(2l_T + 1)} \frac{\pi}{4k_0^2 k_1 k_2} \sum_S (2S + 1) \int_0^\infty dk_1 \int_0^\infty dk_2 \delta\left(\alpha - \tan^{-1} \frac{k_2}{k_1}\right) |\beta|^2 \quad (1)$$

where  $\alpha$  is the hyper-spherical angle between  $\mathbf{k}_1$  and  $\mathbf{k}_2$ ,  $(w_l, l_T)$  are the occupation number and angular momentum of the target subshell, and  $S$  is the total spin of the electrons.

The term  $\beta$  contains all angular dependent terms and phase shifts, and can be written as:

$$\beta = \sum_{L,l_1,l_2} \frac{i^{L+l_1+l_2}}{4\pi} \sum_{M=-1}^{+1} \sum_{m'_j=-1}^{+1} \left( \overbrace{|a_{+1}^L| e^{-i\varepsilon} D_{m'_j,+1}^{J=1}(\omega_{C \rightarrow L}) - |a_{-1}^L| e^{+i\varepsilon} D_{m'_j,-1}^{J=1}(\omega_{C \rightarrow L})}^{P\text{-state of Atom Rotated to } \mathbf{k}_0 \text{ Direction}} \right) \delta_{M,m'_j} \quad (2)$$

$$\times (-1)^{l_1+l_2} \sqrt{(2l_1+1)(2l_2+1)} e^{i(\sigma_{l_1}+\sigma_{l_2})} e^{i(\delta_{l_1}+\delta_{l_2})} \times P_{l_1 l_2}^{L,S}(k_1, k_2, T) \times B_{LM}^{l_1 l_2}(\hat{k}_1, \hat{k}_2)$$

where  $|a_{\pm 1}^L|$  are the amplitudes of the laser-excited target,  $D_{m'_j, \pm 1}^{J=1}(\omega_{C \rightarrow L})$  are rotation matrices that rotate the laser-excited target state into the collision geometry,  $\varepsilon$  defines the alignment angle of the atom in the laser frame,  $\sigma_l, \delta_l$  are Coulomb and distorted wave phase shifts,  $B_{LM}^{l_1 l_2}(\hat{k}_1, \hat{k}_2)$  are bipolar harmonics [8] and  $P_{l_1 l_2}^{L,S}(k_1, k_2, T)$  are time-dependent propagation operators [7].

For the geometry shown in figure 4(c), the laser-excited P-state in the collision frame is given by:

$$|\psi\rangle_{n^1 P_1}^{Las} = \frac{1}{\sqrt{2}} \left( e^{-i\varepsilon} |1,+1\rangle^{Las} - e^{+i\varepsilon} |1,-1\rangle^{Las} \right) = -\frac{i}{\sqrt{2}} \left( |1,+1\rangle^{Las} + |1,-1\rangle^{Las} \right)^{\varepsilon=90^\circ} \quad (3)$$

By substituting equation (3) into equation (2) and by adopting the symmetries that are inherent in the bipolar harmonics, it can be shown that equation (2) reduces to:

$$\beta = \sum_{L,l_1,l_2} \underbrace{\left( 1 - (-1)^{L+l_1+l_2} \right)}_{(\eta)} \frac{(-i)^{L+l_1+l_2+1} (-1)^{L+1} \sqrt{(2l_1+1)(2l_2+1)}}{4\pi\sqrt{2}} B_{L,+1}^{l_1 l_2}(\hat{k}_1, \hat{k}_2) e^{i(\sigma_{l_1}+\sigma_{l_2}+\delta_{l_1}+\delta_{l_2})} P_{l_1 l_2}^{L,S}(k_1, k_2, T) \quad (4)$$

Under these conditions, if  $L+l_1+l_2=2n$  (i.e. if this sum is *even*) then  $\eta=0 \Rightarrow \beta=0$ , and so the QDCS is identically zero. These are called the *natural parity terms*.

By contrast, if  $L+l_1+l_2=2n+1$  (i.e. if this sum is *odd*) then  $\eta=2 \Rightarrow \beta \neq 0$ , and so the QDCS is non-zero. These are called the *unnatural parity terms*. **It is these terms that give rise to the non-zero QDCS that is shown in figure 5(d).**

A similar derivation can be undertaken for the experimental conditions where the P-state is fully aligned in the scattering plane (as in figures 3 and 5(b)). Under these conditions, it is found that only the *natural parity terms* are non-zero, and so for these geometries there is zero contribution to the QDCS from unnatural parity terms. In general for a P-state aligned out of the scattering plane (as in figure 5(c)) it is necessary to include *both* natural and unnatural parity terms in the calculation of the cross sections.

## 5. Future work and conclusions

The model calculations shown in figure 5 demonstrate that the time-independent distorted wave models of the interaction are missing terms that produce the finite cross-section found in the experiments. The TDCC calculation shows that these missing terms are those of unnatural parity. It is important to understand how these terms can be included in time-dependent models, since their use is widespread in modeling plasmas.

Figure 5(a) shows that all models accurately predict the cross-section for the spherically symmetric ground state, and that it is only for the aligned excited targets that substantial differences are found between models. The experiments show that the cross-sections from unnatural parity contributions are substantial (~50% of those from the natural parity states) and so it is important that these terms are included in any models of the ionization of excited targets. Since many plasmas contain large numbers of excited atoms, it is hence likely that current plasma kinetic models are badly underestimating their importance.

Further work is hence being undertaken to clarify how both natural and unnatural parity terms contribute to the ionization cross sections. Since the  $\beta$ -term in equation (2) is a *coherent* summation over different partial waves, it becomes possible to manipulate their different contributions to this sum by choosing different experimental geometries. To facilitate this, the (e,2e) spectrometer in Manchester is being modified to allow the laser beam to be injected into the interaction region from a range of directions with respect to the scattering plane. In this spectrometer it is also possible to move the incident electron beam so that it is lifted out of the detection plane in the experiments. This then changes the relative angles of the scattered and ejected electrons with respect to the collision-frame quantization axis. In this way the sensitivity of the QDCS to the coherent superposition of different partial wave contributions can be manipulated and explored. Both types of experiments will be carried out in collaboration with theoretical input, to determine the sensitivity of the cross-sections to these different conditions.

### References

- [1] M S Pindzola, F Robicheaux, S D Loch, J C Berengut, T Topcu, J Colgan, M Foster, D C Griffin, C P Ballance, D R Schultz, T Minami, N R Badnell, M C Witthoef, D R Plante, D M Mitnik, J A Ludlow and U Kleiman, *J Phys B* **40** (2007) R39
- [2] D H Madison and O Al-Hagan *J At Mol Opt Phys* **2010** (2010) 367180
- [3] K L Nixon and A J Murray *Phys Rev Lett* **112** (2014) 023202
- [4] A D Stauffer *Phys Rev A* **89** (2014) 032710
- [5] S Amami, A J Murray, A Stauffer, K L Nixon, G S J Armstrong, J Colgan and D H Madison, *Phys Rev A* **90** (2014) 062707
- [6] K L Nixon and A J Murray *Phys Rev Lett* **106** (2011) 123201
- [7] G S J Armstrong, J Colgan, M S Pindzola, S Amami, D H Madison, J Pursehouse, K L Nixon and A J Murray *Phys Rev A* **92** (2015) 032706
- [8] H Klar & M Fehr *Z Phys D* **23** (1992) 295